MARY KAY O'CONNOR PROCESS SAFETY CENTER
TEXAS A&M ENGINEERING EXPERIMENT STATION

22nd Annual International Symposium
October 22-24, 2019 | College Station, Texas

Modelling of the plume rise phenomenon due to warehouse fires considering penetration of the mixing layer

Hans Boot and Sonia Ruiz Pérez*
Gexcon AS – Fire and Explosion Consultants
Utrecht, The Netherlands
*Presenter E-mail: sonia.ruiz.perez@gexcon.com

Abstract

The present paper describes the theory behind the "plume rise from warehouse fires model" as implemented in the software package EFFECTS. This model simulates the rising of buoyant plumes due to the density difference between the hot combustion products and the ambient air. The plume rise model calculates the maximum height at which the released material will be in equilibrium with the density of the air, and presents the resulting trajectory of the plume, including hazard distances to specific concentration threshold levels. These parameters will be determined depending on the windspeed, atmospheric stability class and the fire's convective heat production, leading to potential penetration of the mixing layer.

Additionally, the 'penetration fraction' is assessed which expresses the amount of plume penetrating the mixing layer. If the convective heat of production is sufficient to penetrate the mixing layer, the smoke plume will be trapped above the mixing layer. When this occurs, the (potentially toxic) combustion products do not disperse back below the mixing layer, thus, the individuals at ground level are not exposed to the harmful combustion products. If the convective heat of production is not sufficient to penetrate the mixing layer, the smoke plume may experience the so-called reflection phenomena which will trap the smoke plume below the mixing layer. This could have more dangerous consequences for individuals who then might be exposed to harmful combustion products at ground level.

Moreover, this paper includes the validation of the model against experimental data as well as to other widely validated mathematical models. The experiments and mathematical models used for the validation are described, and a detailed discussion of the results is included, with a statistical and graphical comparison against the field data.

Keywords: Consequence Analysis, Modeling, Combustion, Dispersion, Effects, Emission, Gas Dispersion, Plumes, Safety.

1 Introduction

Smoke plumes containing toxic combustion products resulting from warehouse fires, will initially rise due to the density difference between the hot combustion products and the ambient air. This density difference is caused by the fact that the temperature of the plume is significantly higher than the temperature of ambient air. The theory behind this plume rise phenomenon foresees that there will be a height at which the released material will be in equilibrium with the density of the air at that height, leading to a maximum plume height. The trajectory of the plume and the hazard distances to specific concentration threshold levels will be mainly influenced by the windspeed, atmospheric stability class and the fire's convective heat production, where the combination of these parameters lead to potential penetration of, or even reflection by the mixing layer.

Typical models that describe the mathematics behind rising of hot plumes include the effects of atmospheric turbulence, as described by the Pasquill stability class. However, the plume's potential penetration of the mixing layer should also be considered. The importance of the plume penetration is that all mass that has risen above the mixing layer, will never disperse back into the mixing layer. Therefore, toxic combustion products will be trapped above the mixing layer height and will never create chemical exposure at ground level. The reason for this is that at the boundary of the mixing layer (at the temperature inversion height) there is no vertical turbulence. Only the stronger chimney emissions are likely to penetrate upwards due to their greater buoyancy forces. Apart from penetration of the mixing layer height, the potential reflection of the plume should also be considered, which can play a role for plumes that remain below the mixing layer height.

The present study has led to the implementation of a dedicated model, implemented in Gexcon's software package EFFECTS, to simulate the plume rise phenomenon due to warehouse fires. This model calculates the maximum height and plume path of the plume and includes reporting of a 'penetration fraction'. Additionally, the reflection phenomenon is also considered. The model also presents concentration threshold contours of toxic combustion products at any height level.

The model provides safety professionals with valuable information for hazard identification, safety analysis and emergency planning. For instance, if a warehouse fire has enough convective heat production, a toxic smoke plume may rise high enough and even penetrate the mixing layer, not providing any danger at ground level. Trying to extinguish the fire, would decrease the heat production, leading to more danger of toxic exposure at ground level.

Because harmful concentrations may reach very large distances, where the assumption of a homogeneous wind-field is no longer realistic, the plume rise model has also been extended to account for the meandering of the plume (due to time and location dependent meteorological conditions). This model extension uses real-time meteorological data retrieved from the internet, which results in time dependent concentration contours of the plume and a real time view of the meandering plume path. This extension has not been made commercially available but could – when properly integrated into control rooms – provide valuable information to emergency services during interventions.

2 Methodology

2.1 Plume rise modelling

The "plume rise from warehouse fires model" as implemented in the software package EFFECTS is based on Briggs' study of the plume rise phenomenon [1], the theory in the Yellow Book [2] and uses Mill's correction for burning fires [3].

2.1.1 Briggs model

The rising of the plume with distance and the maximum height of the plume can be calculated in two different ways, depending on the atmospheric stability.

For Pasquill stability class A, B, C and D, the rising of the plume with distance and the maximum height of the plume can be calculated with Equation 1, Equation 2 and Equation 3, respectively. The corresponding distance to the maximum height of the plume (x_f) can be calculated with Equation 4 and Equation 5, depending on the value of the initial heat flux (Q_0).

if $x < x_f$ $$h_{BRIGGS} = z_s + 1.6 \cdot Q_0^{\frac{1}{3}} \cdot u_w(z_s)^{-1} \cdot x^{\frac{2}{3}}$$ Equation 1

if $x \geq x_f$ $$h_{BRIGGS} = z_s + 1.6 \cdot Q_0^{\frac{1}{3}} \cdot u_w(z_s)^{-1} \cdot x_f^{\frac{2}{3}}$$ Equation 2

$$h_{max} = z_s + 1.6 \cdot Q_0^{\frac{1}{3}} \cdot u_w(z_s)^{-1} \cdot x_f^{\frac{2}{3}}$$ Equation 3

$$x_f = 49 \cdot Q_0^{\frac{5}{8}} \qquad \text{for } Q_0 < 55$$ Equation 4

$$x_f = 119 \cdot Q_0^{\frac{2}{5}} \qquad \text{for } Q_0 \geq 55$$ Equation 5

For Pasquill stability class E and F, the rising of the plume with distance and the maximum height of the plume can be calculated with Equation 6 and Equation 7, respectively. The Brunt-Vaisala frequency (N) is described in paragraph 2.3.2. The 2/3 relation results from treating the time average profile of the bent over plume as an extension of the model of Morton, 1956 [4].

$$h_{BRIGGS} = z_s + 2 \cdot Q_0^{\frac{1}{3}} \cdot u_w(z_s)^{-\frac{1}{3}} \cdot N^{-\frac{2}{3}} \cdot \left(1 - \cos\frac{N \cdot x}{u_w(z_s)}\right)^{\frac{1}{3}}$$ Equation 6

$$h_{max} = z_s + 2.52 \cdot Q_0^{\frac{1}{3}} \cdot u_w(z_s)^{-\frac{1}{3}} \cdot N^{-\frac{2}{3}}$$ Equation 7

2.1.2 Mills correction for burning fires

According to Zonato et al, 1999 [5] the assessment of the rising of smoke plumes resulting from free burning fires would be appropriate by implementing a series of relations as suggested by Mills, 1987 [3]. Mills suggested altering the Briggs formula as shown in the equation below, where

h_{BRIGGS} corresponds to the plume rise due to buoyancy effects as described in the Briggs model (see paragraph 2.1.1).

$$h_{MILLS} = \left[(h_{BRIGGS})^3 + \left(\frac{D}{2 \cdot \gamma}\right)^3\right]^{\frac{1}{3}} - \frac{D}{2 \cdot \gamma}$$ Equation 8

Additionally, Mills described the initial heat flux (Q_0) as follows:

$$Q_0 = (1 - 0.3) \cdot 0.037 \cdot Q_H$$ Equation 9

Mills assumes that the 30% of the heat released in the combustion is dispersed as thermal radiation in the surrounding area and that the 70% of the heat combustion is devoted to the plume rise. Consequently, the term $[(1 - 0.3) \cdot Q_H]$ corresponds to the convective heat flux. Moreover, the term $[D/2 \cdot \gamma]$ is inserted in the Briggs formula (where $\gamma = 0.6$ is the entrainment coefficient for a buoyant plume rise) to account for the initial diameter of the plume, which is considered equal to the extent of the fire.

2.2 Calculation of the plume concentration

In order to calculate the concentration of the plume, it is necessary to know not only the position of the plume centerline but also the way in which the material is distributed through the plume's width and height. A rising plume entrains air into its own volume, thereby, increasing its radius. A rising plume is also subject to the normal processes of turbulent diffusion which acts to increase the plume size. The standard deviation of the distribution should allow for the effects of plume rise and passive diffusion on plume growth (as described in paragraph 2.2.3).

The Gaussian Plume Model as described in the Yellow Book [2] can be applied to describe passive dispersion if the dispersing cloud is either neutral or positively buoyant. Therefore, the Gaussian Plume Model is selected to calculate the dispersion phenomena for all scaling regions in the mixing layer. The Gaussian Plume Model is valid for dispersion calculations over flat, uniform terrain. The gaussian mathematical equations have been extended to account for reflection of the plume material in the mixing height (as described in paragraph 2.2.1).

The general expression to calculate the plume concentration (in kg/m^3) for continuous releases is:

$$C(x, y, z) = \frac{q_F}{u_w(z_c)} \cdot F_y(x, y) \cdot F_z(x, z)$$ Equation 10

Where q_F is the formation rate of the chemical of interest (i.e. C, CO_2, HBr, HCl, HF, NO_2 or SO_2) and $u_w(z_c)$ the wind velocity at the plume centerline. The expression $F_y(x,y)$ accounts for lateral (crosswind) dispersion (see paragraph 2.2.1) and $F_z(x,z)$ accounts for vertical dispersion (see paragraph 2.2.1). Because of the importance of the source rate of a specific toxic combustion product, this formation rate of the chemical of interest can be calculated with the EFFECTS model "combustion and toxic combustion products". This combustion model allows for the calculation of the combustion of solid and liquid products due to warehouse fires, based on a gross chemical structural formula and burning area.

2.2.1 Lateral (crosswind) dispersion

The expression $F_y(x,y)$ accounts for the lateral (crosswind) dispersion and it is calculated as shown in Equation 12 and Equation 13. The calculation of lateral dispersion depends on the initial source half dimension in the lateral direction (b_{oy}), which is assumed to be the initial radius of the fire.

$$b_{oy} = \frac{D}{2}$$ Equation 11

If $b_{oy} = 0$…

$$F_y(x,y) = \frac{1}{\sqrt{2 \cdot \pi} \cdot \sigma_y(x)} \cdot e^{-\frac{y^2}{2 \cdot \sigma_y^2(x)}}$$ Equation 12

If $2 \cdot b_{oy} > 0$…

$$F_y(x,y) = \frac{1}{4 \cdot b_{oy}} \cdot \left\{ \operatorname{erf}\left(\frac{b_{oy} - y}{\sqrt{2} \cdot \sigma_y(x)} \right) + \operatorname{erf}\left(\frac{b_{oy} + y}{\sqrt{2} \cdot \sigma_y(x)} \right) \right\}$$ Equation 13

2.2.2 Vertical dispersion

The expression $F_z(x,z)$ accounts for the vertical dispersion and it is calculated as shown in the equations below. The calculation of vertical dispersion depends on the source half dimension in the vertical direction (b_{oz}), which is also assumed to be the initial radius of the fire.

$$b_{oz} = \frac{D}{2}$$ Equation 14

The calculation of the vertical dispersion depends on several parameters:

- **Penetration fraction:**
  The penetration fraction P(x) is the fraction of mass that has risen above the mixing layer height and it is calculated assuming a gaussian distribution of mass in the vertical direction. The penetration fraction might increase with distance until the maximum plume height h_{max} is reached. Additionally, the penetration fraction will reach its maximum value at the distance where the maximum height of the plume is reached. The significance of the penetration fraction is that this mass fraction can never expose a risk a ground level. A value of P = 0.5 implies that half the plume is above the mixing layer height, whereas P = 1 implies full penetration. It is assumed that at the top of the mixing layer, there is a region (at the temperature inversion height) where there is no vertical turbulence. That means that there is no turbulent exchange of mass through this inversion layer height.

  $$P(x) = \frac{1}{2} + \frac{1}{2} \cdot \operatorname{Erf}\left(\frac{h_{max} - MH}{\sqrt{2} \cdot \sigma_z(X_d)} \right)$$ Equation 15

The vertical dispersion parameter of the smoke plume (σ_z) needs to be calculated for the distance at which the height of study is reached by the cloud. Therefore, the expression in Equation 16 can be used where X_d corresponds to the addition of the distance at which the height of study of the plume is reached (x_f) to the distance of a virtual source (V_z). See paragraph 2.3.1 for more information about the virtual source.

$$X_d = x_f + V_z$$ Equation 16

- **Reflection**:
  Reflection is the phenomenon in which concentrations get "bounced back" against a non-penetrable boundary, such as the ground level or temperature inversion layer. For plumes near the ground level, the reflection against the ground (R_G) needs to be accounted for. For plumes near the mixing layer height the reflection against the mixing layer (R_{MH}) needs to be considered. The mixing layer acts as a ceiling for the smoke plume.

The calculation of the vertical dispersion needs to consider two different situations: (1) vertical dispersion when the plume is no longer rising, hence, it has reached its maximum height (see paragraph 2.2.2.1); (2) vertical dispersion when the plume is still rising, and has not yet reached its maximum height (see paragraph 2.2.2.2).

2.2.2.1 Plume has reached its maximum height

Once the plume has reached its maximum height, the plume center line can be situated either below or above the mixing layer height.

<u>If $h_{max} < MH$</u>

If the maximum height of the plume is situated <u>below the mixing layer height</u>, the penetration fraction is expected to be small (as shown in the left picture of Figure 1) or 0 (as shown in the right picture of Figure 1). This is typically because the plume does not have sufficient momentum to penetrate the mixing layer due to its heat of combustion. In this situation the reflection of the plume against the mixing layer height needs to be accounted for.

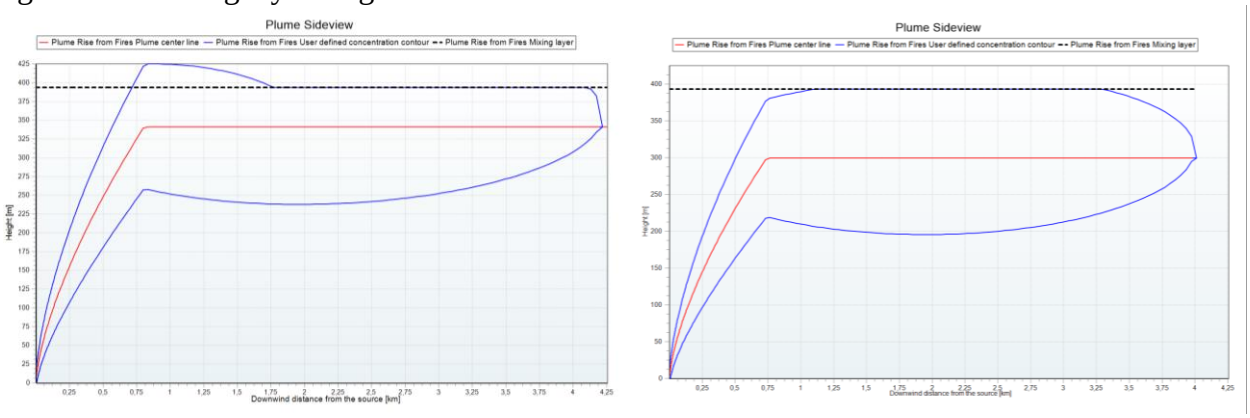

Figure 1. Plume with a maximum height situated below the mixing layer height with a very small penetration fraction (left) and with no penetration (right)

In order to be able to describe the full trajectory of the plume, the calculation needs to include two different approaches to calculate the vertical dispersion depending on whether the vertical coordinate of study is below or above the mixing layer height for every distance evaluated.

- If $z < MH$

  When the vertical coordinate of study is situated below the mixing layer height, and $P < l$, the plume will not fully penetrate the mixing layer. In this case, the reflection from the mixing layer height (R_{MH}) and from the ground (R_G) need to be incorporated.

$$F_z(x,z) = \frac{1}{\sqrt{2\cdot\pi}\cdot\sigma_z(x)}\cdot\exp\left[-\frac{(z-z_c)^2}{2\cdot\sigma_z^2(x)}\right] + R_G + CF\cdot R_{MH} \qquad \text{Equation 17}$$

  Where:

$$R_G = \frac{1}{4\cdot b_{oz}}\cdot\left\{\operatorname{erf}\left(\frac{b_{oz}-z-z_c}{\sqrt{2}\cdot\sigma_z(x)}\right) + \operatorname{erf}\left(\frac{b_{oz}+z+z_c}{\sqrt{2}\cdot\sigma_z(x)}\right)\right\} \qquad \text{Equation 18}$$

$$CF = P(x) - P(x_f) \qquad \text{Equation 19}$$

$$R_{MH} = \frac{1}{\sqrt{2\cdot\pi}\cdot\sigma_z(x)}\cdot\left\{\exp\left(-\frac{(z-z_{c,reflected})^2}{2\cdot\sigma_z^2(x)}\right) + \exp\left(-\frac{(z+z_{c.reflected})^2}{2\cdot\sigma_z^2(x)}\right)\right\} \qquad \text{Equation 20}$$

$$z_{c,reflected} = 2\cdot MH - h_{max} \qquad \text{Equation 21}$$

- If $z \geq MH$

  When the vertical coordinate of study is situated above the mixing layer height, and the plume has partly penetrated the mixing layer, a different situation occurs. In this case, the reflection from the mixing layer height (R_{MH}) and from the ground (R_G) does not need to be included, because the upper part of the plume will only dilute upwards.

$$F_z(x,z) = \frac{1}{\sqrt{2\cdot\pi}\cdot\sigma_z(x)}\cdot\exp\left[-\frac{(z-z_c)^2}{2\cdot\sigma_z^2(x)}\right]\cdot CF \qquad \text{Equation 22}$$

$$\text{If } P(x) > 0 \quad CF = \frac{P(x_f)}{P(x)} \qquad \text{Equation 23}$$

$$\text{If } P(x) \leq 0 \quad CF = 0 \qquad \text{Equation 24}$$

<u>If $h_{max} \geq MH$</u>

If the maximum height of the plume is situated <u>above the mixing layer height</u>, then $P > 0.5$. In this case, the penetration fraction needs to be evaluated, because it is highly relevant for the dilution of the plume concentration. In the situation where $P = 1$, the smoke plume will be fully trapped above the mixing layer (see left picture in Figure 2), hence, the (toxic) combustion products will not

disperse back below the mixing layer. However, in some other cases the plume will not fully penetrate the mixing layer (P < 1). Therefore, for the mass fraction below mixing layer, reflection against the ground needs to be taken into account (see right picture in Figure 2).

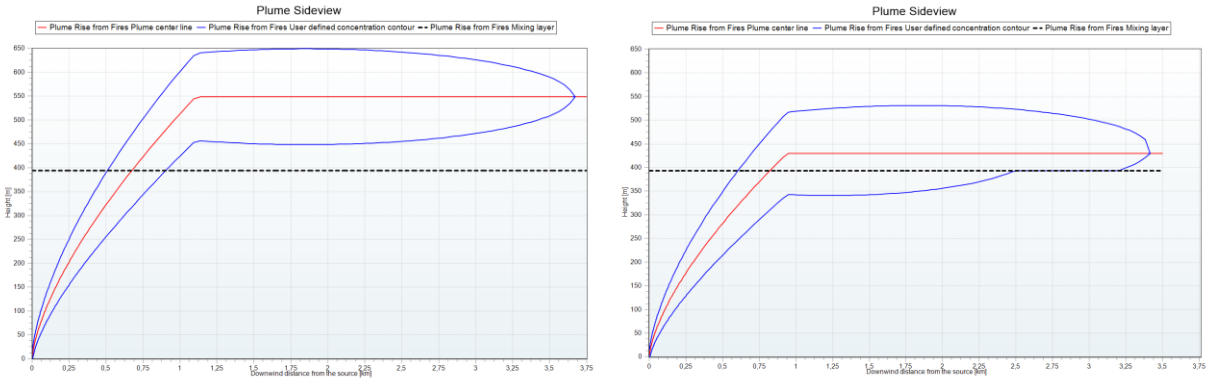

Figure 2. Plume with a maximum height situated above the mixing layer height with full penetration (left) and partial penetration (right)

In order to be able to describe the full trajectory of the plume, the calculation needs to include two different approaches to calculate the vertical dispersion depending on whether the vertical coordinate of study is below or above the mixing layer height for every distance evaluated.

- If z < MH

  When the vertical coordinate of study is situated below the mixing layer height and P < 1, the plume will not fully penetrate the mixing layer. In this case, the reflection from the ground (R_G) need to be evaluated for the mass fraction that has not penetrated the mixing layer. However, the reflection from the mixing layer height (R_{MH}) does not need to be included because the maximum height of the plume is already above the mixing layer height, where this reflection phenomena will not occur.

$$F_z(x,z) = CF \cdot \left(\frac{1}{\sqrt{2 \cdot \pi} \cdot \sigma_z(x)} \cdot \exp\left[-\frac{(z - z_c)^2}{2 \cdot \sigma_z^2(x)} \right] + R_G \right) \quad \text{Equation 25}$$

$$\text{If } P(x) < 1 \quad CF = \frac{1 - P(x_f)}{1 - P(x)} \quad \text{Equation 26}$$

$$\text{If } P(x) \geq 1 \quad CF = 0 \quad \text{Equation 27}$$

- z ≥ MH

  When the vertical coordinate of study is situated above the mixing layer height, the plume will fully or partly penetrate the mixing layer. This is typically because the plume does have enough momentum to penetrate the mixing layer due to its heat of combustion. In this case, the reflection from the mixing layer height (R_{MH}) needs to be evaluated because it is possible that not all the plume penetrates though the mixing layer. However, the reflection from the ground (R_G) does not need to be considered because the vertical coordinate of study is above the mixing layer height, hence, this phenomenon is not relevant.

$$F_z(x,z) = \frac{1}{\sqrt{2 \cdot \pi} \cdot \sigma_z(x)} \cdot \exp\left[-\frac{(z - z_c)^2}{2 \cdot \sigma_z^2(x)}\right] + CF \cdot R_{MH}$$ Equation 28

In this case, the correction factor (CF) is calculated in the same way as expressed in Equation 19, the height of the reflected centerline of the plume ($z_{c,reflected}$) is calculated as expressed in Equation 21, and the reflection against the mixing layer height (R_{MH}) is calculated as indicated in the equation below.

$$R_{MH} = \frac{1}{\sqrt{2 \cdot \pi} \cdot \sigma_z(x)} \cdot \left\{\exp\left(-\frac{\left(MH + z_{c,reflected}\right)^2}{2 \cdot \sigma_z^2(x)}\right) + \exp\left(-\frac{\left(MH - z_{c,reflected}\right)^2}{2 \cdot \sigma_z^2(x)}\right)\right\}$$ Equation 29

2.2.2.2 Plume is rising

While the plume is rising, the penetration fraction might still be increasing as a function of distance. The only correction required in the calculation of vertical dispersion is the reflection against the ground (R_G). This is because any part of the plume reaching this mixing layer boundary, will always penetrate through the mixing layer height due to the density differences.

Additionally, a calculation approach is used when the vertical coordinate of study is below the centerline of the plume. This allows the plume rise model to separate the penetrating behavior of the fraction of the plume that is below the centerline of the cloud, from the fraction of the plume above the centerline of the cloud.

$$F_z(x,y) = \frac{1}{\sqrt{2 \cdot \pi} \cdot \sigma_z(x)} \cdot \exp\left[-\frac{(z - z_c)^2}{2 \cdot \sigma_z^2(x)}\right] + R_G$$ Equation 30

2.2.3 Crosswind and vertical wind dispersion parameters

The purpose of the crosswind (σ_y) and vertical wind (σ_z) dispersion parameters of the smoke plume is to account for dilution in the crosswind and vertical wind directions. The reflection of the plume at the ground can be accounted for by assuming an image source at distance "x" beneath the ground surface. These dispersion parameters can be calculated as follows.

$$\sigma_y(x) = \left(\frac{t'}{600}\right)^{0,2} \cdot a \cdot {X_d}^b$$ Equation 31

$$\sigma_z(x) = (10 \cdot z_0)^{0,53 \cdot {X_d}^{-0,22}} \cdot c \cdot {X_d}^d$$ Equation 32

For a, b, c and d the values according to the following table are applicable [2]:

Pasquill Class	a	b	c	d
Very unstable (A)	0.527	0.865	0.28	0.90
Unstable (B)	0.371	0.866	0.23	0.85
Slightly unstable (C)	0.209	0.897	0.22	0.80
Neutral (D)	0.128	0.905	0.20	0.76
Stable (E)	0.098	0.902	0.15	0.73
Very stable (F)	0.065	0.902	0.12	0.67

Table 1. Value of the parameters a, b, c and d depending on the Pasquill stability class

2.3 Ad-hoc formulas

2.3.1 Virtual source

The concept of virtual source is included in the plume rise model to account for the initial area of the warehouse fire. The virtual source corresponds to a point located below ground level and back from the actual source location that gives an equivalent horizontal cross-sectional area to the actual source (V_y) and an equivalent vertical cross-sectional area to the actual source (V_z). The parameters a, b, c and d can be chosen as described in paragraph 2.2.3.

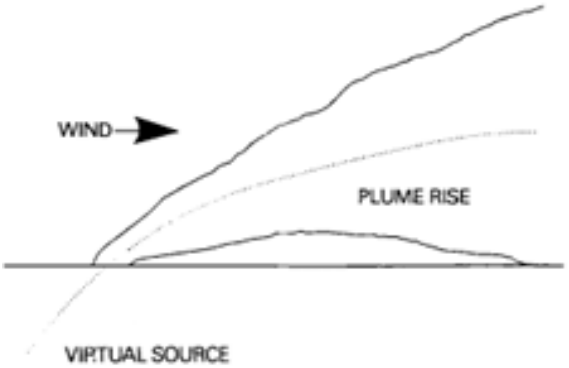

Figure 3. Graphic representation of a virtual source as depicted in Carter, 1989 [6]

$$V_y = \left(0.5 \cdot \frac{D}{a}\right)^{\frac{1}{b}}$$ Equation 33

$$V_z = \left(0.5 \cdot \frac{D}{c}\right)^{\frac{1}{d}}$$ Equation 34

2.3.2 Brunt-Vaisala frequency

The Brunt-Vaisala frequency (N) can be calculated for Pasquill stability class E and F using the data in Table 2.

$$N = \sqrt{\frac{g}{T_a} \cdot \left(\frac{\partial T_a}{\partial z} + 0.01\right)}$$ Equation 35

Pasquill stability class	$\delta T_a/\delta z$ ($K \cdot m^{-1}$)	Average N
E	-0.005 to 0.015	0.005
F	Bigger than 0.015	0.028

Table 2. Average Brunt-Vaisala frequency according to the Pasquill stability class

2.3.3 Inverse Monin-Obukhov length

The Inverse Monin-Obukhov length (1/L) can be calculated for different stability classes using the data in Table 3.

$$\frac{1}{L} = \frac{1}{L_{MO}} \cdot \log_{10}\left(\frac{z_0}{Z_{MO}}\right)$$ Equation 36

Pasquill stability class	L_{MO} [m]	Z_{MO} [m]
A	33,162	1117
B	32,258	11,46
C	51,787	1,324
D	∞	Not applicable
E	-48,330	1,262
F	-31,325	19,36

Table 3. Constants needed for the calculation of the inverse Monin-Obukhov length

2.3.4 Mixing layer height

The atmospheric mixing layer height (MH) is usually capped by a sharp elevated inversion which blocks dispersion of substances emitted near the ground from mixing further upwards.

Pasquill stability class	1/L	MH [m]
E, F	>0	$0.4 \cdot \sqrt{u_* \cdot L/f}$
D	0	$\min(0.2 \cdot u_*/f, 500)$
C	<0	1000
B		1500
A		1500

Table 4. Calculation of the mixing layer height according to the Pasquill stability class

Where Equation 37 is used to calculate frequency and Equation 38 to calculate friction velocity.

$$f = 2 \cdot \Omega \cdot \sin\phi$$ Equation 37

$$u_* = k \cdot \frac{u_w(z_{10})}{f\left(\frac{z_{10}}{z_0}, L\right)}$$ Equation 38

The velocity functions are calculated as follows. Note that if z>100m then z=100m must be used.

$$\begin{cases} f\left(\frac{z_{10}}{z_0}, L\right) = \ln\frac{z_{10}}{z_0} + 5 \cdot \frac{(z_{10}-z_0)}{L} & \text{for } \frac{1}{L} > 0 \\ f\left(\frac{z_{10}}{z_0}, L\right) = \ln\frac{z_{10}}{z_0} - \Psi\left(\frac{z_{10}}{L}\right) + \Psi\left(\frac{z_0}{L}\right) & \text{for } \frac{1}{L} \leq 0 \end{cases}$$ Equation 39

$$\Psi\left(\frac{z}{L}\right) = 2 \cdot \ln\left(\frac{1+\Psi'}{2}\right) + \ln\left(\frac{1+\Psi'^2}{2}\right) - 2 \cdot \arctan(\Psi') + \frac{\pi}{2}$$ Equation 40

$$\Psi' = \left(1 - 16 \cdot \frac{z}{L}\right)^{\frac{1}{4}}$$ Equation 41

2.3.5 Wind speed at height of study

According to the Nieuw Nationaal Model [7] the wind speed at a height of study can be calculated as follows.

$$u_w(z) = u_w(z_{10}) \cdot \frac{\ln\left(\frac{z}{z_0}\right) - \Psi\left(\frac{z}{L}\right) + \Psi\left(\frac{z_0}{L}\right)}{\ln\left(\frac{z_{10}}{z_0}\right) - \Psi\left(\frac{z_{10}}{L}\right) + \Psi\left(\frac{z_0}{L}\right)}$$ Equation 42

Depending on whether the inverse Monin-Obukhov length (1/L) is positive or negative, the empirical functions are described differently.

- If $L < 0$

$$\Psi\left(\frac{z}{L}\right) = 2 \cdot \ln\left(\frac{1+\Psi'}{2}\right) + \ln\left(\frac{1+\Psi'^2}{2}\right) - 2 \cdot \arctan(\Psi') + \frac{\pi}{2}$$ Equation 43

$$\Psi' = \left(1 - 16 \cdot \frac{z}{L}\right)^{\frac{1}{4}}$$ Equation 44

- If $L \geq 0$

$$\Psi\left(\frac{z}{L}\right) = -17 \cdot \left(1 - e^{\frac{-0.29 \cdot z}{L}}\right)$$ Equation 45

The value of z in the empirical function ψ (z/L) can be substituted by the surface roughness length (z_0), a stack height of 10 m (z_{10}) or the height of study (z), depending on which empirical function needs to be used.

3 Validation

The validation of the "plume rise from warehouse fires model" is performed by comparing the results given with EFFECTS with measurements from field experiments and with other already validated mathematical models. The validation includes a description of each validation experiment and a detailed discussion of the results obtained from a statistical and graphical comparison against the field data.

Each experiment set is statistically evaluated to determine the accuracy and precision of the "plume rise from warehouse fires model" model predictions versus the observed data. The fraction of predictions within a factor of two of the measurements is analyzed and represented in a scatter plot. Note that the quantitative acceptance criteria for FAC2 is that $0.5 \leq \text{FAC2} \leq 2$ (see Equation 46).

$$0.5 \leq \left(\text{FAC2} = \frac{C_p}{C_m}\right) \leq 2 \qquad \text{Equation 46}$$

3.1 Validation of the concentration

The investigation presented by Hall, Kukadia, Walker & Marsland [8] is used to validate the concentration of the rising plume as implemented in EFFECTS. This investigation examines a variety of fire plume discharges in a small-scale wind tunnel. For more information about the experimental conditions please refer to the original literature as presented by Hall, Kukadia, Walker & Marsland [8].

The following figure shows experimental ground level concentrations downwind of the source for discharges with buoyancy only, where S, T, U, V, W, and X correspond to different experimental data which represent different buoyancy conditions. The validation in Figure 4 shows that the simulation of S, T, U, V and W present good agreement with the experimental data. The simulation of X shows over-predicted values for downwind distances very close to the source.

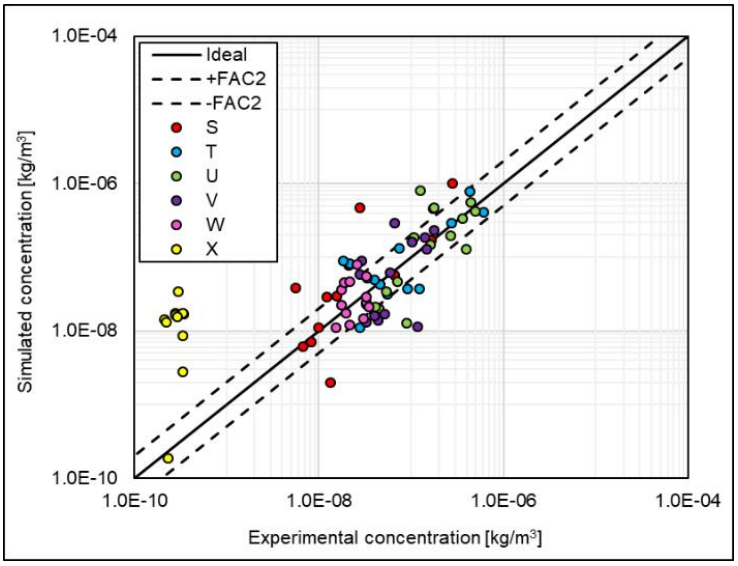

Figure 4. Validation of the Gexcon's model against Hall's experimental data. Buoyancy only

The following figure shows experimental ground level concentrations downwind of the source with a combination of buoyancy and discharge momentum. W1, W2, W3, W4, X1, X2, Y1, and Y2 correspond to different experimental data which represent different conditions of buoyancy and momentum flux. The validation in Figure 5 shows that the simulation of W1, W2, W4 and X1 present good agreement with the experimental data. The simulation of W3, X2, Y1 and Y2 show under-predicted values for downwind distances relatively close to the source.

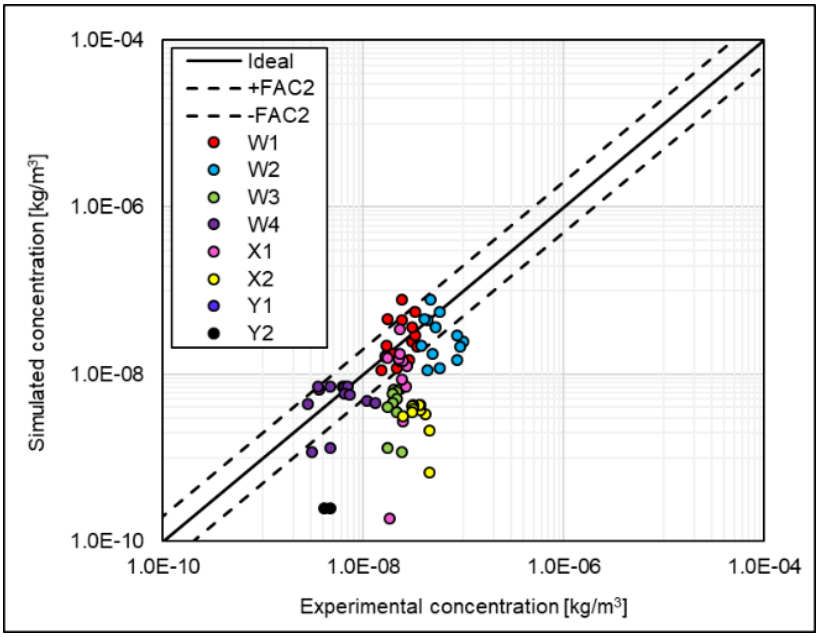

Figure 5. Validation of Gexcon's model against Hall's experimental data. Buoyancy & momentum

3.2 Validation of the plume height

Briggs [1] collected a series of experimental data for rising plumes, namely: Harwell, Bosanquet, Darmstadt, Duisburg, Tallwarra, Lakeview, CEGB plants, Earley, Castle Donington, Northfleet, TVA plants, Shawnee, Colbert, Johnsonville, Widows Creek, Gallatin and Paradise. The already validated theoretical formulas listed below, are used to assess EFFECTS' performance against this experimental data and compared with other validated theoretical formulas to calculate the maximum height of the plume.

- Moses & Carson, 1967
  Moses & Carson [9] developed a formula for ten different stacks. The least-squares fit was given by the empirical equation described in the equation below.

$$h_{max} = 1.81 \left[\frac{ft^2/s}{(cal/s)^{1/2}} \right] \cdot \frac{Q_H^{\frac{1}{2}}}{u_w(z_s)} \qquad \text{Equation 47}$$

- Stümke, 1963
  Stümke [14] derived the empirical formula described in Equation 48, on the basis of data from four stacks, namely, the Harwell stack [10-11], Moses and Strom's experimental stack [12], and the two stacks reported by Rauch [13].

$$h_{max} = 1.5 \cdot \left(\frac{w_0}{u_w(z_s)}\right) \cdot D + 118 \left[\frac{m^{\frac{1}{2}}}{s}\right] \cdot D^{\frac{3}{2}} \cdot \left(1 + \frac{\Delta T}{T_s}\right)^{\frac{1}{4}} \cdot u_w(z_s)^{-1} \qquad \text{Equation 48}$$

- Holland

  The equation for the calculation of the plume rise phenomenon developed by Holland was developed based on photographs taken at three steam plants near Oak Ridge, Tennessee [15]. Holland found the best fit to the data with the empirical equation detailed in Equation 49.

$$h_{max} = 1.5 \cdot \left(\frac{w_0}{u_w(z_s)}\right) \cdot D + 4.4 \cdot 10^{-4} \left[\frac{ft^2/s}{cal/s}\right] \cdot \frac{Q_H}{u_w(z_s)} \qquad \text{Equation 49}$$

- Priestley

  Priestley [16] developed Equation 50 which assumes that atmospheric turbulence dominates the mixing while plume rise occurs.

$$h_{max} = 2.7 \left[\left(\frac{ft}{s}\right)^{\frac{1}{4}}\right] \cdot F^{\frac{1}{4}} \cdot u_w(z_s)^{-1} \cdot x^{\frac{3}{4}} \qquad \text{Equation 50}$$

- Lucas, Moore & Spurr

  Lucas, Moore & Spurr [17] fitted observed plume rises at two of their plants with Equation 51. The formula is based on a simplification of Priestley's theoretical plume-rise model.

$$h_{max} = 258 \left[\frac{ft^2/s}{(cal/s)^{\frac{1}{4}}}\right] \cdot \frac{Q_H^{\frac{1}{4}}}{u_w(z_s)} \qquad \text{Equation 51}$$

- Lucas

  Lucas [18] noted some correlation with stack height and suggested a modification of the equation developed by Lucas, Moore & Spurr. This equation (see Equation 52) is not suited to plants with heat emission less than 10 MW because it predicts continued plume rise to almost 1 km downwind regardless of source size.

$$h_{max} = (134 + 0.3 \cdot z_s) \left[\frac{ft^2/s}{(cal/s)^{\frac{1}{4}}}\right] \cdot \frac{Q_H^{\frac{1}{4}}}{u_w(z_s)} \qquad \text{Equation 52}$$

- Briggs, 1969

  Briggs developed a theoretical model to predict penetration of a sharp elevated inversion of height through which the temperature increases. For the first stage of the rise, the bent-over model predicts the centerline for buoyant plumes in neutral conditions and it is given by the expression in Equation 53. This equation, which corresponds to Equation 4.32 in Briggs' publication [1], can be used up to the distance at which atmospheric turbulence dominates entrainment.

$$h_{max} = 1.8 \cdot F^{\frac{1}{3}} \cdot u_w(z_s)^{-1} \cdot x^{\frac{2}{3}}$$ Equation 53

Once the distance at which atmospheric turbulence dominates entrainment is reached (x^*), the following equation can be used to simulate the complete plume centerline. This equation should not be applied beyond $x = 5 \cdot x^*$, because so few data go beyond this distance. This equation corresponds to Equation 4.34 in Briggs' publication [1].

$$h_{max} = 1.8 \cdot F^{\frac{1}{3}} \cdot u_w(z_s)^{-1} \cdot x^{*\frac{2}{3}} \cdot \left[\frac{2}{5} + \frac{16}{25} \cdot \frac{x}{x^*} + \frac{11}{5} \cdot \left(\frac{x}{x^*}\right)^2\right] \cdot \left(1 + \frac{4}{5} \cdot \frac{x}{x^*}\right)^{-2}$$ Equation 54

The validation in the figure below shows that the simulation of the plume rise phenomenon with the "plume rise from warehouse fires model" as implemented in EFFECTS present very good agreement with experimental data. Moreover, from all the theoretical formulas collected in the publication of Briggs [1] and described in the present study, the equations implemented in EFFECTS (described in chapter 2**Error! Reference source not found.**) present the best agreement with experimental data.

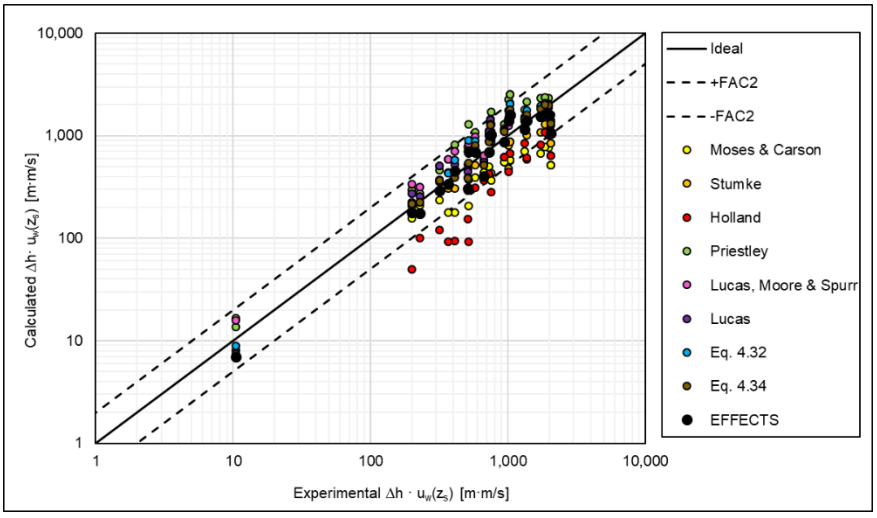

Figure 6. Validation of Gexcon's model against the already validated theoretical formulas

On the other hand, the formulas of Moses & Carson (Equation 47), Stümke (Equation 48) and Holland (Equation 49) are completely empirical and do not allow for the effect of distance of measurement on plume rise as the other formulas do. Consequently, these three formulas give poorer agreement with data. The Holland formula (Equation 49) shows a high percentage of scatter. Priestley's formula (Equation 50) is an asymptotic formula which predicts a rise proportional to $x^{¾}$. This is a transitional-rise formula which shows less scatter compared with observations than the formulas of Moses & Carson, Stümke and Holland. Lucas, Moore & Spurr's formula (Equation 51) includes both a transitional and a final-rise stage and gives a little better agreement with experimental data. When Lucas, Moore & Spurr's formula is multiplied by the empirical stack-height factor suggested by Lucas (Equation 52), the agreement is considerably better. Brigg's formula (Equation 53) is based on the "2/3 law", which is another transitional-rise formula, and agrees well with the experimental data. The other Brigg's formula (Equation 54),

which includes both a transitional-rise and a final-rise stage, gives both improved numerical agreement and much less percentage of scatter.

4 Results

In this chapter the results obtained with the "plume rise from warehouse fires model" as implemented in the software package EFFECTS are presented. For all the figures included in this chapter, the **black dashed line** corresponds to the mixing layer height, the **red line** corresponds to the centerline of the rising plume and the **dark green line** corresponds to the side view contour for a threshold concentration of 1 mg/m^3. The **dark blue line**, **light green line** and **pink line** correspond to the side view contour for a threshold concentration corresponding to PAC-1, PAC-2 and PAC-3 of Carbon (soot); respectively.

4.1 Plume penetrating the mixing layer

In the left picture of Figure 7 an example is given for a fully penetrating plume (P = 1) calculated with EFFECTS. In this case, soot is the pollutant being evaluated which comes from a fire with a convective heat of production of 30 MW. The soot formation rate at those conditions is 0.28 kg/s. The Pasquill stability class evaluated is D2 (neutral). The roughness length description is based on scattered large objects.

In the right picture of Figure 7 an example is given for a fully penetrating plume (P = 1) calculated with EFFECTS which experiences reflection from the mixing layer which prevents the (toxic) combustion products to disperse below the mixing layer. In this case, the same conditions as the previous example are used, except from the fire's convective heat of production which is reduced to 20 MW.

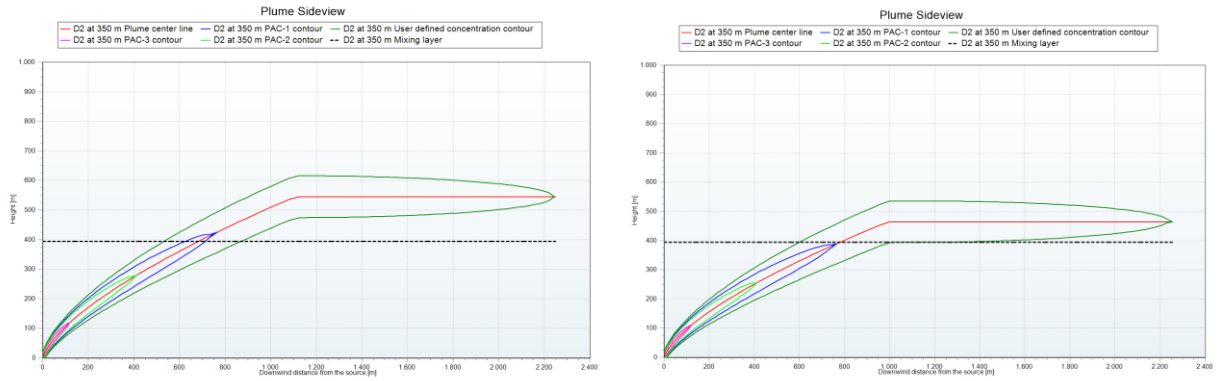

Figure 7. Plume fully penetrating the mixing layer (P = 1) without R_{MH} (left) and with R_{MH} (right)

In the left picture of Figure 8 an example is given for a partly penetrating plume (P < 1) calculated with EFFECTS which experiences reflection from the mixing layer upon penetration. In this case, the same conditions as the previous example are used, except from the fire's convective heat of production which is reduced to 5 MW.

In the right picture of Figure 8 an example is given for a partly penetrating plume (P = 0.5) calculated with EFFECTS which experiences reflection from the ground in the fraction of the plume that remains below the mixing layer height. In this case, the same conditions as the previous example are used, except from the fire's convective heat of production which is reduced to 4 MW. As it can be seen from the figure below the mixing layer is located at the same height as the plume centerline.

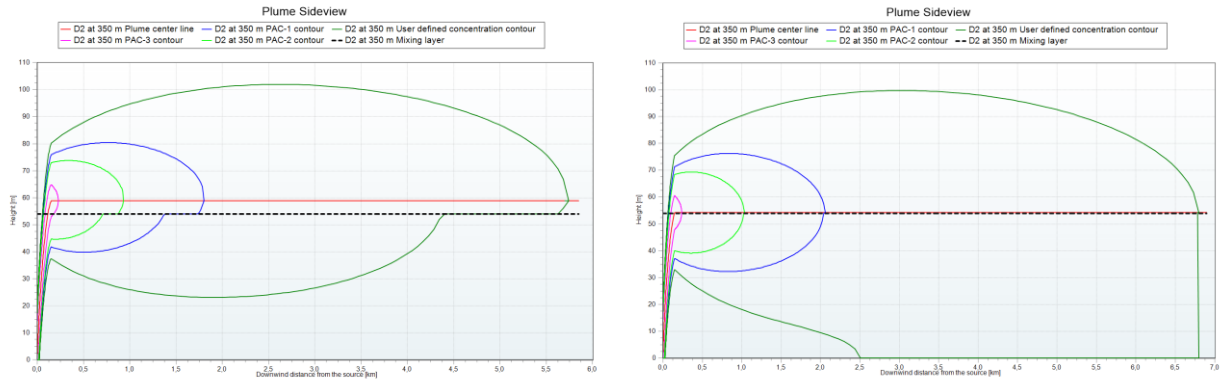

Figure 8. Plume partly penetrating the mixing layer (P < 1) with R_{MH} (left) and with R_G (right)

4.2 Plume non-penetrating the mixing layer

In the left picture of Figure 9 an example is given for a non-penetrating plume (P = 0) calculated with EFFECTS. In this case, the same conditions as the previous example are used, except from the fire's convective heat of production which is increased to 10 MW and the atmospheric stability is changed to D2 (neutral).

In the right picture of Figure 9 an example is given for a non-penetrating plume (P = 0) calculated with EFFECTS which experiences reflection from the ground. In this case, the same conditions as the previous example are used, except from the fire's convective heat of production which is reduced to 1 MW.

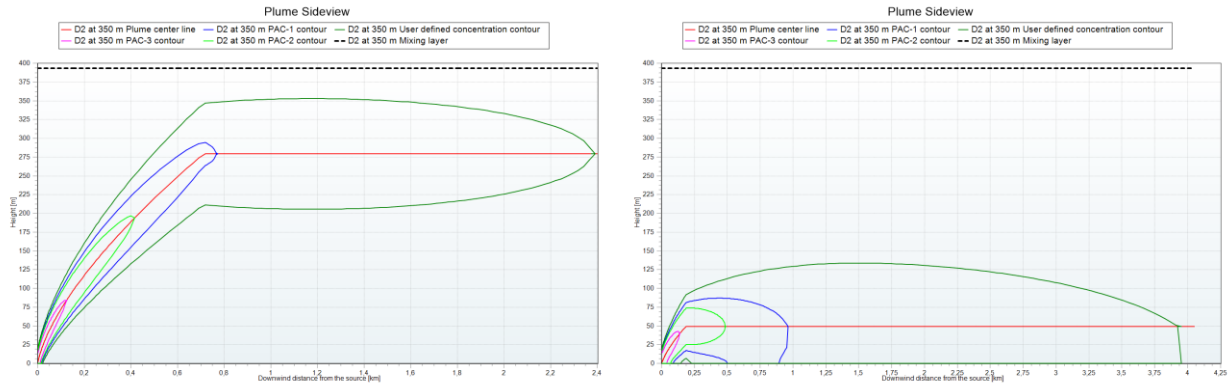

Figure 9. Plume not penetrating the mixing layer (P = 0) without reflection (left) and with R_G (right)

5 Conclusions and future work

5.1 Conclusions

The “plume rise from warehouse fires model” is a model implemented in the software package EFFECTS to calculate the plume rise phenomenon due to warehouse fires. The model is based on the theory presented on Briggs’ study [1], the theory in the Yellow Book [2] and corrected with Mill’s correction for burning fires [3].

Additionally, a mathematical approach for the calculation of the potential penetration of the plume through the atmospheric mixing layer has been developed by Gexcon and implemented in EFFECTS. This modelling approach allows the modeler to include in the calculations of plume rise, that all mass that has risen above the mixing layer, will never disperse back into the mixing layer. Therefore, for such conditions, (toxic) combustion products will never create chemical exposure at ground level.

Furthermore, another mathematical approach has been included to simulate the reflection phenomena which will “trap” the smoke plume below or above the mixing layer. This phenomenon is highly relevant because if the plume is “trapped” below the mixing layer, there could be more severe consequences for individuals at ground level exposed to toxic combustion products.

The “plume rise from warehouse fires model” has been extensively validated against experimental data and against other widely used and validated mathematical models. The results of the simulations with the “plume rise from warehouse fires model” as implemented in EFFECTS, present not only very good agreement with experimental data but also the best agreement compared to other already validated mathematical formulas.

5.2 Future work

The warehouse fire phenomenon creates a toxic combustion product plume that can affect a very large area. Nevertheless, the traditional “homogeneous wind-field” dispersion modelling of such a toxic plume can become unreliable because of the potential long distance of dangerous concentrations (>10 km). At these long distances, the wind direction and wind velocity may have changed, as these atmospheric parameters are not constant at every location and height.

The “plume rise from warehouse fires model” uses a homogenous wind field. However, the toxic plume will show a meandering behavior and may bend into different directions at different heights or after some time.

For this reason, the “plume rise from warehouse fires model” has been extended to account for the meandering of the plume due to time and location dependent meteorological conditions. This

extension, called the “dynamic plume rise model”, uses on-line meteorological data and has been implemented as a web-based GIS tool, called RESPONSE.

RESPONSE is currently available as a demonstrator and uses real-time meteorological data to calculate actual and realistic hazard zones of a chemical accident. If properly integrated into control rooms, RESPONSE could allow emergency response organizations to immediately evaluate potential hazard zones, and to make well-founded decisions on alarming, evacuation and repression actions that will minimize social disruption, and potential damage to people, constructions and infrastructure.

Experimental data and previous experience with this phenomenon show that warehouse fires rarely produce hazardous concentrations at environment level. This is caused by the fact that the plume rise effect will usually force the fumes high up in the sky, potentially penetrating the mixing layer. This maximum height of the plume is highly influenced by the heat production and combustion efficiency of the fire. Firemen may try to extinguish the fire, which leads to less plume rise behavior. Therefore, feedback on the resulting plume height is very important to potentially correct the plume path and concentration predictions. In order to do this, access to sensor data, information from drones or observation reports could be connected to the modelling to make predictions more reliable.

The RESPONSE framework is intended for its integration as an additional module into existing Emergency Services GIS environments. Hence, it should be customized towards the specific user, who can define dedicated accident scenarios and use specific hazard level contours.

In the figure below, it is depicted the RESPONSE interface illustrating a meandering smoke plume, using location and time specific wind field.

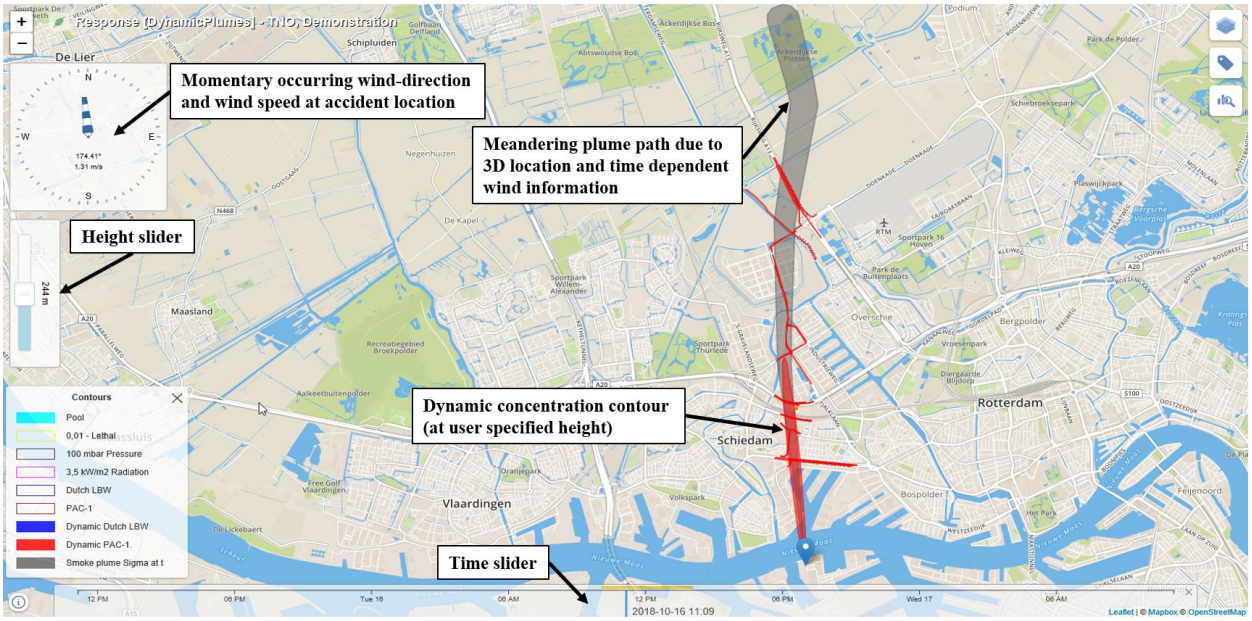

Figure 10. RESPONSE demonstrator showing a dynamic smoke plume using time specific wind field

6 Nomenclature

a, b, c, d	Constant parameters that depend on the Pasquill stability class (Table 1)	[-]
b_{oy}	Source half dimension in crosswind direction	[m]
b_{oz}	Source half dimension in vertical direction	[m]
C(x,y,z)	Downwind concentration at coordinate (x, y, z)	[kg/m^3]
CF	Correction factor	[-]
C_m	Measured (experimental) value	NA
C_p	Predicted (simulated) value	NA
D	Diameter of the fire / internal stack diameter	[m]
Erf	Gauss error function	[-]
f	Coriolis parameter	[s^{-1}]
F	Buoyancy flux parameter	[m^4/s^3]
F_y (x,y)	Parameter to describe the lateral (crosswind) dispersion	[-]
F_z (x,z)	Parameter to describe the vertical dispersion	[-]
g	Gravity	[m/s^2]
h_{BRIGGS}	Plume rise due to buoyancy according to Briggs	[m]
h_{max}	Maximum height of the plume	[m]
h_{MILLS}	Plume rise according to the Mills correction	[m]
k	Von Karman constant	[0.4]
L	Monin-Obukhov length	[m]
L_{MO}	Constant for the calculation of the Monin-Obukhov length	[m]
MH	Mixing layer height	[m]
N	Brunt-Vaisala frequency	[s^{-2}]
P(x)	Penetration fraction at distance x	[-]
P(x_f)	Penetration fraction at distance x_f	[-]
q_F	Formation rate	[kg/s]
Q_0	Initial heat flux	[kcal/s]
Q_H	Total heat rate	[kcal/s]
R_G	Reflection against the ground	[-]
R_{MH}	Reflection against the mixing layer height	[-]
t’	Averaging time	[s]
T_a	Ambient temperature	[K]
T_s	Average absolute temperature of gases emitted from stack	[K]
u_*	Friction velocity	[m/s]
u_w (z)	Wind speed at height of study	[m/s]

u_w (z_{10})	Wind speed at a height of 10 m	[m/s]
u_w (z_c)	Wind speed at the centerline of the plume	[m/s]
u_w (z_s)	Wind speed at stack height	[m/s]
V_y	Virtual source for vertical cross-section area equivalent to actual source	[m]
V_z	Virtual source for horizontal cross-section area equivalent to actual source	[m]
w_0	Efflux speed of gases from stack	[m/s]
x	Downwind distance	[m]
x^*	Distance at which atmospheric turbulence dominates entrainment	[m]
x_f	Downwind distance at which the plume reaches its maximum height	[m]
X_d	$x_f + V_z$	[m]
y	Crosswind horizontal coordinate	[m]
z	Vertical upward coordinate or height of study	[m]
z_0	Surface roughness length	[m]
z_{10}	Height of 10 m	[m]
z_c	Plume centerline	[m]
$z_{c,reflected}$	Height of the reflected centerline of the plume	[m]
z_s	Stack height	[m]
Z_{MO}	Constant for the calculation of the Monin-Obukhov length	[m]
ΔT	Temperature excess of stack gases	[K]
γ	Entrainment coefficient for buoyant plume rise	[-]
σ_y (x)	Crosswind dispersion parameter of the cloud	[m]
σ_z (x)	Vertical dispersion parameter of the cloud	[m]
ϕ	Earth's latitude	[°N]
Ψ(z/L)	Empirical function	[-]
Ψ'	Empirical function	[-]
Ω	Earth's rotational speed ($7.27 \cdot 10^{-5}$)	[s^{-1}]

7 References

[1] Briggs, G. Plume Rise. Air Resources Atmospheric Turbulence and Diffusion Laboratory. Environmental Science Services Administration. Oak Ridge, Tennessee. 1969.

[2] Yellow Book. Methods for the calculation of physical effects due to release of hazardous materials (liquids and gases). CPR14E. 2nd Edition, 1992. The Hague, The Netherlands.

[3] M.T. Mills. Modelling the release and dispersion of toxic combustion products from chemical fires. International Conference on Vapor Cloud Modelling. November 1987. Boston, Massachusetts.

[4] Morton, B., Taylor, G., & Turnen, J. Turbulent Gravitational Convection from Maintained and Instantaneous Sources. Proceedings of the Royal Society of London. 234: 1-23. 1956. London, UK.

[5] C. Zonato, A. Vidili, R. Pastorino and D.M. de Faveri. Plume rise of smoke coming from free burning fires. Journal of Hazardous Materials, 34: 69-79. 1993. November 28, 1991. Italy.

[6] Carter, D. Methods for estimating the dispersion of toxic combustion products from large fires. Chemical Engineering Research & Design. 67: 348-352. 1989.

[7] TNO Milieu, Energie en Procesinnovatie. Het Nieuwe Nationaal Model. Model voor de verspreiding van luchtverontreiniging uit bronnen over korte afstanden. Apeldoorn, 1998. TNO Rapportnummer RR 98/306.

[8] Hall, D., Kukadia, V., Walker, S., & Marsland, G. Watford. Plume dispersion from chemical warehouse fires. Building Research Establishment. UK, 1995.

[9] Moses, H., & Carson, J. Stack design parameters influencing plume rise. 60th Annual Meeting of the Air Pollution Control Association. 67-84. Cleveland, Ohio, 1967.

[10] Stewart, N., Gale, H., & Crooks. The atmospheric diffusion of gases discharged from the chimney of the Harwell Pipe (BEPO). British Report AERE HP/R-1452, R-1954.

[11] Stewart, N., Gale, H., & Crooks. The atmospheric diffusion of gases discharged from the chimney of the Harwell reactor (BEPO). International Journal of Air and Water Pollution. 87-102. R-1958.

[12] Moses, H., & Strom, G. A comparison of observed plume rises with values obtained from well-known formulas. Journal of Air Pollution. 455-466. 1961.

[13] Rauch, H. Zur Schornstein - Überhöhung. Beiträge zur Physik der Atmosphäre, 37: 132-158. Translated in USAEC Report ORNL-tr-1209. 1964.

[14] Stümke, H. Suggestions for an empirical formula for chimney elevation. Oak Ridge National Laboratory, 23: 549-556. Translated in USAEC Report ORNL-tr-977. 1963.

[15] A meteorological survey of the Oak Ridge Area: Final report covering the period 1948-1952. USAEC Report ORO-99. U.S. Weather Bureau. 554-559. 1953.

[16] Priestley, H. A working theory of the bent-over plume of hot gas. Quarterly Journal of the Royal Meteorology Society, 82: 165-176. 1956.

[17] Lucas, D., Moore, D., & Spurr, G. The rise of hot plumes from chimneys. International Journal of Air and Water Pollution, 7: 473-500. 1963.

[18] Lucas, D. Application and evaluation of results of the Tilbury plume rise and dispersion experiment. Journal of Atmospheric Environment, 1: 421-424. 1967.